

Figure 1. A heat map of tumors in the genomic grade index (GGI) and prognosis study is shown. One hundred five tumors were subjected to gene expression analysis. (A) Columns of the heat map correspond to 97 genes used for GGI analysis, and rows of the heat map correspond to individual tumors, which were sorted first by histological grade (HG) 1, HG2, or HG3, and then by GGI within each histological grade category. In the heat map, high expression is red and low expression is green. (B) GGI score of each tumor is plotted on the right side of the corresponding row of heat map. (C) The prognosis of patients with each tumor is shown. Red represents patients with recurrence, and blue represents those without recurrence. L indicates low; H, high.

genomic grade index tumors. Relations between genomic grade index and the various clinicopathological parameters are shown in Table 1, indicating that high genomic grade index tumors were more likely to be large, PR negative, HER2 positive, and Ki67 positive.

The recurrence-free survival (RFS) rate for patients with high genomic grade index tumors was significantly ($P < .001$) lower than for those with low genomic grade index tumors (55% vs 88%, 10 years after surgery) (Fig. 2A). After classification of the 62 histological grade 2 tumors into high genomic grade index and low genomic grade index tumors, the RFS rates for the patients with these tumors were compared (Fig. 2B). The rate for patients with high genomic grade index tumors was significantly ($P = .012$) lower than for those with low genomic grade index tumors (54% vs 83%, 10 years after surgery), indicating that genomic grade index can help to clearly differentiate high-risk from low-risk tumors even among histological grade 2 tumors.

Comparison of Genomic Grade Index With Other Prognostic Factors for the Prediction of RFS Rates

Association of various conventional prognostic factors with RFS was analyzed by means of univariate analysis

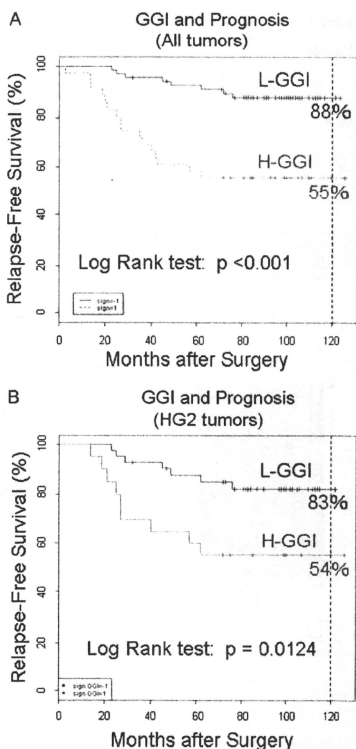


Figure 2. Recurrence-free survival curves are shown (A) for all patients ($n = 105$) and (B) for patients with histological grade 2 tumors ($n = 62$) according to genomic grade index (GGI). L indicates low; H, high; HG2, histological grade 2.

(Table 2), and it was found to be significant between high recurrence rates and large tumor size, high histological grade, or positive HER2. Moreover, high genomic grade index was significantly ($P < .001$) associated with a high recurrence rate. Multivariate analysis demonstrated that genomic grade index was the most important and significant predictive factor for disease recurrence ($P = .013$) independently from other, conventional prognostic factors.

Table 2. Univariate and Multivariate Analysis of Various Prognostic Factors

Factor	Univariate ^a				Multivariate ^a			
	Hazard Ratio	Lower 95% CI	Upper 95% CI	P	Hazard Ratio	Lower 95% CI	Upper 95% CI	P
Mens	1.79	0.80	4.04	.160	1.49	0.60	3.68	.390
T	2.49	1.22	5.05	.012	1.72	0.88	3.37	.110
HG	2.71	1.08	6.84	.035	1.49	0.49	4.17	.520
PR	0.51	0.20	1.30	.160	0.63	0.22	1.80	.390
HER2	2.84	1.21	6.65	.016	1.80	0.72	4.46	.210
Ki67	1.69	0.67	4.26	.270	0.65	0.22	1.89	.430
GGI	2.22	1.45	3.39	<.001	1.86	1.14	3.05	.013

CI indicates confidence interval; Mens; menstruation; T, tumor size; HG, histological grade; PR, progesterone receptor; HER2, human epidermal growth receptor 2; GGI; genomic grade index.

^aCox proportional hazard model.

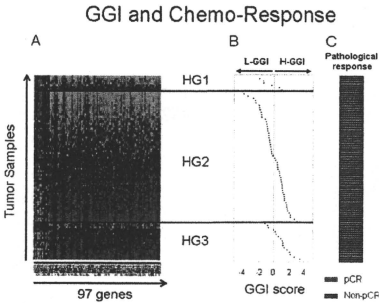


Figure 3. A heat map of tumors in the genomic grade index and chemoresponse study is shown. Eighty-four tumors were subjected to gene expression analysis. (A) Columns in the heat map correspond to 97 genes used for genomic grade index (GGI) analysis, and rows in the heat map correspond to individual tumors, which were sorted first by histological grade (HG) 1, HG2, or HG3, and then by GGI within each HG category. In the heat map, high expression is red and low expression is green. (B) The GGI score of each tumor is plotted on the right side of the corresponding row of heat map. (C) The pathological response to neoadjuvant chemotherapy (paclitaxel followed by 5-fluorouracil/epirubicin/cyclophosphamide) of each tumor is shown. Red represents pathological complete response (pCR), and blue represents non-pCR. L indicates low; H, high.

Genomic Grade Index and Response to Chemotherapy

The gene expression profile of the tumor biopsy samples ($n = 84$) obtained before neoadjuvant chemotherapy (P-FEC) were analyzed by means of DNA microarray for classification into high genomic grade index and low genomic grade index tumors (Fig. 3). Of the 7 histological grade 1 tumors, 5 (71.4%) were classified into low genomic grade index tumors, and of the 17

histological grade 3 tumors, 14 (82.4%) were classified into high genomic grade index tumors. Of the 60 histological grade 2 tumors, 29 (48.3%) were classified into low genomic grade index tumors and 31 (51.7%) into high genomic grade index tumors.

The pathological CR rate to P-FEC was significantly ($P = .022$) higher for high genomic grade index (31.9%) tumors than low genomic grade index tumors (10.8%) (Table 3). The subset analysis according to ER status showed that the pathological CR rate was higher for high genomic grade index tumors than low genomic grade index tumors both in the ER-positive subset (17.4% vs 4.0%) and in the ER-negative subset (45.8% vs 25.0%), although the difference was not statistically significant.

Disease-free survival of these 84 patients according to genomic grade index is shown in Figure 4 (median follow-up period, 28 months; range, 1-56 months). There was no significant difference in RFS between high genomic grade index tumors and low genomic grade index tumors.

DISCUSSION

In the study presented here, we evaluated the prognostic value of genomic grade index for lymph node-negative and ER-positive breast cancer patients treated with adjuvant hormonal therapy alone. We were able to demonstrate that in the case of Japanese breast cancers, most histological grade 3 tumors can be classified into high genomic grade index tumors and most histological grade 1 tumors into low genomic grade index tumors, as was previously reported for Caucasian breast cancers. High genomic grade index tumors were more likely to be ER negative, PR negative, HER2 positive, and Ki67 positive, and are thus considered to possess a biologically aggressive phenotype. Accordingly, prognosis for high genomic

Table 3. Relationship Between GGI and pCR Rates for Neoadjuvant Chemotherapy

	No. of Tumors	pCR Rate		<i>P</i> ^a
		H-GGI	L-GGI	
Total	84	31.9%	10.8%	.022
ER positive	48	17.4%	4.0%	.129
ER negative	36	45.8%	25.0%	.227

GGI indicates genomic grade index; pCR, pathological complete response; H-GGI, high-GGI; L-GGI, low-GGI.

^a Chi-square test.

grade index tumors was significantly poorer than for low genomic grade index tumors, and more importantly, histological grade 2 tumors could be clearly differentiated into high genomic grade index tumors with poor prognosis and low genomic grade index tumors with good prognosis. All these findings for the association between genomic grade index and prognosis for Japanese breast cancers are consistent with those reported for Caucasian breast cancer patients, indicating that genomic grade index determined by the 97-gene signature for molecular classification of breast tumors is a statistically robust method regardless of ethnicity.

Because prognosis for lymph node-negative and ER-positive breast tumors is usually estimated by using tumor size, histological grade, PR, HER2, and more recently Ki67, it seems important to compare genomic grade index with these conventional prognostic parameters to determine the independent prognostic value of genomic grade index. However, such a comparison has never been done in previously reported studies. We therefore conducted a multivariate analysis of genomic grade index and conventional prognostic factors and were able to show that genomic grade index is a highly significant prognostic factor independent of the other, conventional prognostic factors. These results seem to indicate that genomic grade index would be very useful for decision making as to whether adjuvant chemotherapy should be added to adjuvant hormonal therapy for lymph node-negative and ER-positive breast cancers.

Prognostic signatures (MammaPrint and Oncotype DX) other than genomic grade index have also been reported, and all these signatures appear to have a similar prognostic performance, but are likely to be limited to ER-positive tumors.⁸ The common and most prominent characteristic among these prognostic signatures is the high expression of the genes responsive for cell proliferation. Ki67 is the most reliable marker for cell proliferation among those currently available, and we have been able to

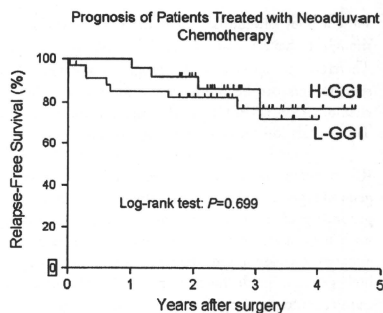


Figure 4. Prognosis of breast cancer patients treated with neoadjuvant chemotherapy is shown. Recurrence-free survival curves of 84 patients treated with neoadjuvant chemotherapy (paclitaxel followed by 5-fluorouracil/epirubicin/cyclophosphamide) are shown according to genomic grade index (GGI). H indicates high; L, low.

show that, as expected, high genomic grade index tumors are associated with Ki67-positive tumors. However, we believe that the prognostic value of genomic grade index is stronger than that of Ki67, because the multivariate analysis has clearly shown that genomic grade index is most strongly associated with prognosis independently of other parameters, including Ki67. These results seem to suggest that genomic grade index can identify cell proliferation more accurately than Ki67 or that genomic grade index can identify not only cell proliferation but also other biological features related to metastases.

Because high genomic grade index tumors are associated with high proliferation, and highly proliferating tumors can be expected to respond well to chemotherapy, we also investigated, as part of this study, the association of genomic grade index with pathological CR rates in the neoadjuvant setting, and were able to show that high genomic grade index tumors are significantly ($P = .022$) associated with a high pathological CR rate. This tendency was also observed in the ER-positive tumor subset. These results are essentially consistent with those reported very recently by Liedtke et al, who have shown that high genomic grade index breast cancer tumors are associated with a high pathological CR rate to neoadjuvant chemotherapy consisting of paclitaxel followed by 5-fluorouracil/doxorubicin/cyclophosphamide.⁴ All these results taken together indicate that, in the lymph node-negative and ER-positive subset, high genomic grade index tumors

show a poor prognosis, but at the same time they are thought to have a relatively higher sensitivity to P-FEC. Therefore, it is speculated that prognosis of patients with such tumors can be improved by addition of adjuvant chemotherapy (P-FEC) to adjuvant hormonal therapy. This speculation needs to be proven in future study.

We found that there was no significant difference in RFS between high genomic grade index tumors and low genomic grade index tumors (Fig. 4). Because high genomic grade index tumors have a worse baseline prognosis as compared with low genomic grade index tumors, a modest increase in sensitivity to P-FEC associated with high genomic grade index tumors might be unable to translate into the improvement of their prognosis over low genomic grade index tumors. Interestingly, Liedtke et al reported that high genomic grade index tumors showed a worse prognosis than low genomic grade index tumors in the ER-positive subset.⁴ Therefore, it is considered that genomic grade index modestly predicts chemosensitivity in patients who receive neoadjuvant chemotherapy, but its impact on prognosis still remains to be clarified.

In the prognosis study of 105 patients, we used poly-T primers for RNA amplification, but in the chemoresponse study of 84 patients, we used the Ovation method (random primers) because of a small sample volume of Mammotome specimens. It is possible that determination of genomic grade index would be affected by the different chemical approaches to RNA amplification.^{9,10} However, concordance between histological grade 1 and low genomic grade index and between histological grade 3 and high genomic grade index was similarly high both in the prognosis study (37 of 43, 86%) and in the chemoresponse study (19 of 24, 79%), suggesting that genomic grade index results obtained using the Ovation method would be comparable to those obtained using poly-T primers.

In conclusion, we were able to show that genomic grade index is a very strong prognostic factor for lymph node-negative and ER-positive tumors independently of the currently available prognostic biomarkers, including PR, HER2, and Ki67, and that high genomic grade index tumors are more likely to respond to chemotherapy (P-FEC). Thus, genomic grade index seems to represent a helpful diagnostic tool for decision making as to the addition of adjuvant chemotherapy to adjuvant hormonal therapy for this subset of breast tumors. Very recently, Toussaint¹¹ et al reported that they succeeded in the conversion of DNA microarray-based determination of genomic grade index to a quantitative reverse-transcrip-

tase polymerase chain reaction (PCR) assay (PCR-genomic grade index), which can be used for RNA derived from formalin-fixed paraffin-embedded tumor specimens. The methods they have developed seem to have the potential to be widely used for risk assessment of lymph node-negative and ER-positive breast cancers.

CONFLICT OF INTEREST DISCLOSURES

Grants were provided by the Knowledge Cluster Initiative and Scientific Research on Priority Areas programs of the Ministry of Education, Culture, Sports, Science, and Technology of Japan, and by the Comprehensive 10-Year Strategy for Cancer Control program of the Ministry of Health, Labor, and Welfare, Japan.

REFERENCES

- Sotiriou C, Wirapati P, Loi S, et al. Gene expression profiling in breast cancer: understanding the molecular basis of histologic grade to improve prognosis. *J Natl Cancer Inst*. 2006;98:262-272.
- Desmedt C, Giobbie-Hurder A, Neven P, et al. The gene expression grade index: a potential predictor of relapse for endocrine-treated breast cancer patients in the BIG 1-98 trial. *BMC Med Genomics*. 2009;2:40.
- Loi S, Haibe-Kains B, Desmedt C, et al. Definition of clinically distinct molecular subtypes in estrogen receptor-positive breast carcinomas through genomic grade. *J Clin Oncol*. 2007;25:1239-1246.
- Liedtke C, Hatzis C, Symmans WF, et al. Genomic grade index is associated with response to chemotherapy in patients with breast cancer. *J Clin Oncol*. 2009;27:3185-3191.
- Morimoto K, Kim SJ, Tanei T, et al. Stem cell marker aldehyde dehydrogenase 1-positive breast cancers are characterized by negative estrogen receptor, positive human epidermal growth factor receptor type 2, and high Ki67 expression. *Cancer Sci*. 2009;100:1062-1068.
- Tanei T, Morimoto K, Shimazu K, et al. Association of breast cancer stem cells identified by aldehyde dehydrogenase 1 expression with resistance to sequential paclitaxel and epirubicin-based chemotherapy for breast cancers. *Clin Cancer Res*. 2009;15:4234-4241.
- Elston CW, Ellis IO. Pathological prognostic factors in breast cancer. I. The value of histological grade in breast cancer: experience from a large study with long-term follow-up. *Histopathology*. 1991;19:403-410.
- Haibe-Kains B, Desmedt C, Piette F, et al. Comparison of prognostic gene expression signatures for breast cancer. *BMC Genomics*. 2008;9:394.
- Viale A, Li J, Tiesman J, et al. Big results from small samples: evaluation of amplification protocols for gene expression profiling. *J Biomol Tech*. 2007;18:150-161.
- Clement-Ziza M, Gentien D, Lyonnet S, Thiery JP, Besmond C, Decraene C. Evaluation of methods for amplification of picogram amounts of total RNA for whole genome expression profiling. *BMC Genomics*. 2009;10:246.
- Toussaint J, Sieuwerts AM, Haibe-Kains B, et al. Improvement of the clinical applicability of the genomic grade index through a qRT-PCR test performed on frozen and formalin-fixed paraffin-embedded tissues. *BMC Genomics*. 2009;10:424.

Oral fluoropyrimidine may augment the efficacy of aromatase inhibitor via the down-regulation of estrogen receptor in estrogen-responsive breast cancer xenografts

Mamoru Nukatsuka · Hitoshi Saito · Fumio Nakagawa · Masaaki Abe · Junji Uchida · Jiro Shibata · Ken-ichi Matsuo · Shinzaburo Noguchi · Mamoru Kiniwa

Received: 20 April 2010 / Accepted: 18 August 2010
© Springer Science+Business Media, LLC. 2010

Abstract The present preclinical study was designed to evaluate a new combination therapy comprised of the aromatase inhibitor anastrozole (ANA) and the oral fluoropyrimidines, UFT and S-1 against the estrogen receptor (ER)-positive human breast cancer cell line MCF-7/Arom 14, which was stably transfected with the cDNA of human aromatase. MCF-7/Arom 14 cells showed a high aromatase activity and notably were able to grow in the presence of testosterone and estradiol (E₂) in vitro. ANA and 5-fluorouracil (5-FU) inhibited cell growth at concentrations of 0.005–10 and 0.2–5 μM, respectively, and the combination of both drugs additively inhibited cell growth. The growth of MCF-7/Arom 14 tumors was significantly inhibited by ANA and S-1 or UFT in vivo. The combination of ANA with S-1 or UFT administered using a 21-day consecutive, metronomic-like regimen significantly enhanced the antitumor efficacy, suppressing tumor growth for 2–4 times longer than monotherapy. To investigate the mechanisms by which S-1 enhances the antitumor activity of ANA, the protein and mRNA expression levels of ER-α in tumor tissue after treatment with S-1, ANA, and the typical

chemotherapeutic agents doxorubicin (ADM) or paclitaxel (TXL) were analyzed. The protein and mRNA expression levels of ER-α in the tumor tissue were markedly decreased after treatment with S-1 or S-1 + ANA, but not after treatment with either ADM or TXL. The reduced ER-α level after S-1 treatment might contribute to the increased antitumor activity of ANA by reducing ER-α-induced growth signaling in addition to the decrease in estrogen production induced by ANA. Based on these results, the combination of ANA and S-1 might yield a greater benefit than other chemotherapeutic agents in postmenopausal women with ER-positive breast cancer.

Keywords Aromatase inhibitor · Breast cancer · Chemo-endocrine combination therapy · Estrogen receptor · MCF-7/Arom 14 cell · S-1 · UFT

Abbreviations

ANA	Anastrozole
CI	Combination index
DCC	Dextran-coated charcoal-stripped
ADM	Doxorubicin hydrochloride
Ct	Threshold cycle
DIF	DPD inhibitory fluoropyrimidine
DPD	Dihydropyrimidine dehydrogenase
E ₂	17β-Estradiol
ER	Estrogen receptor
5-FU	5-Fluorouracil
FCS	Fetal calf serum
GAPDH	Glyceraldehyde-3-phosphate dehydrogenase
GD	Growth delay
HPMC	Hydroxypropyl methylcellulose
HRP	Horseshoe peroxidase
IC ₅₀	50% Inhibitory concentration

M. Nukatsuka (✉) · H. Saito · F. Nakagawa · M. Abe · J. Uchida · M. Kiniwa
Tokushima Research Center, Taiho Pharmaceutical Co., Ltd.,
224-2, Ebisuno Hirایشi, Kawauchi-Cho, Tokushima-Shi,
Tokushima 771-0194, Japan
e-mail: m-nukatsuka@taiho.co.jp

J. Shibata · K. Matsuo
Hanno Research Center, Taiho Pharmaceutical Co., Ltd., 1-27,
Misugidai, Hanno-Shi, Saitama 357-8527, Japan

S. Noguchi
Department of Breast and Endocrine Surgery, Osaka University
Graduate School of Medicine, 2-2-E10 Yamadaoka Suita, Osaka
565-0871, Japan

TXL	Paclitaxel
RT-PCR	Reverse transcriptional polymerase chain reaction
RTV	Relative tumor volume
S-1	Tegafur-gimeracil-oteracil
TAM	Tamoxifen
Tes-P	Testosterone pellet
TGI	Tumor growth inhibition
UFT	Tegafur-uracil

Introduction

Breast cancer is the most common cancer among women, and several treatment modalities have been aggressively investigated [1]. As in the case with cancer of other organs, the treatment of breast cancer patients has recently tended to be more personalized and detailed as a result of the analysis of various biomarkers, such as hormone receptors (ER/PgR), as well as the HER-2 status and other risk factors. In an adjuvant setting, the details of treatment options for individual patients are frequently discussed and revised [1].

Essentially, adjuvant endocrine therapy is recommended for all hormone receptor-positive breast cancer patients, and the addition of adjuvant chemotherapy to endocrine therapy has been shown to further improve the prognosis of ER-positive breast cancer patients [2]. However, the addition of anthracyclines to adjuvant endocrine therapy has recently been shown to improve the outcome of patients with ER-positive and HER2-positive breast cancer (luminal B) but not the outcome of patients with ER-positive and HER2-negative breast cancer (luminal A) [3]. Hayes et al. also reported an additional benefit of adjuvant paclitaxel (TXL) for patients luminal B but not for those with luminal A [4]. Thus, patients with the luminal A subset are unlikely to benefit from adjuvant chemotherapies including anthracyclines and/or taxanes. As the proportion of luminal A tumors (73.2%) is higher than that of luminal B tumors (13.8%) [5], the development of effective chemoendocrine regimens for the patients with luminal A tumors is urgently needed [6].

In Japan, several clinical studies using an oral dihydropyrimidine dehydrogenase (DPD)-inhibitory fluoropyrimidine (DIF), tegafur-uracil (UFT), have been performed, and the combination of UFT with tamoxifen (TAM) has been demonstrated to improve the overall survival of patients with node-negative and ER-positive tumors, compared with surgery alone [7]. In node-positive patients, UFT combined with TAM was shown not to be inferior to the intravenous cyclophosphamide-methotrexate-fluorouracil regimen in terms of relapse-free survival [8, 9]. In

addition, preliminary results have indicated that UFT confers an additional benefit to TAM alone in an ER-positive and HER2-negative tumor subset [10]. Therefore, a combination chemoendocrine therapy consisting of TAM with UFT might be a promising postoperative treatment option for patients with luminal A-type tumors.

Approximately two-thirds of breast cancers are hormone-responsive, and this proportion is higher among postmenopausal women [1]. In the treatment of postmenopausal patients with advanced diseases, aromatase inhibitors (AI), including anastrozole (ANA), have exhibited a superior survival and toxicity profile compared with the antiestrogen TAM [11–13]. Among the newly developed oral fluoropyrimidines that are being used to treat breast cancer patients, S-1 and capecitabine have been demonstrated to be active as a 2nd or 3rd line therapy for ER-negative breast cancer patients who have failed to respond to anthracycline or taxane therapy; however, the efficacies of these agents in combination with TAM or AI are still under clinical investigation for ER-positive, postmenopausal breast cancer patients.

S-1, unlike capecitabine, is composed of 1 M tegafur (a masked form of 5-FU), 0.4 M gimeracil (a potent inhibitor of the 5-FU degradation enzyme in the liver and tumor tissues), and 1 M potassium oteracil (which mainly inhibits the phosphorylation of 5-FU in the gastrointestinal [GI] tract) [14]. S-1 has been shown to be effective against ER-negative breast cancer (MX-1 and MC-2) and other human cancers *in vivo* [14] and to have a potent antitumor efficacy with a lower GI toxicity for various types of cancers [15, 16]. In particular, S-1 showed a high clinical response rate of about 42% among previously untreated breast cancer patients in a clinical phase II study in Japan [17].

Aromatase is mainly expressed in cancer and stromal cells in the mammary gland and the systemic adipose tissues of postmenopausal patients, while estrogen is supplied from adrenal androgen [18, 19]. However, established human breast cancer cell lines *in vitro* have less aromatase activity than surgically removed breast cancer tissues [20]; moreover, the plasma levels of estrogen and adrenal androgen in mice are reportedly extremely low [21]. To investigate the efficacy of aromatase inhibitor against human breast cancer xenografts in nude mice, we established the ER-positive human breast cancer cell line MCF-7/Arom 14, which stably expresses aromatase as a result of the transfection of human aromatase cDNA, and implanted these cells with the concomitant implantation of a testosterone-releasing pellet (Tes-P) into nude mice. This study describes the characteristics of MCF-7/Arom 14 breast cancer cells *in vitro* and the *in vivo* antitumor efficacy of oral fluoropyrimidines and ANA, either alone or in combination, against such ER-positive breast tumors with high aromatase activity levels.

In this study, we sought to determine whether the co-administration of S-1 and ANA for 3 weeks according to a metronomic-like schedule would be capable of significantly down-regulating the expression of ER- α in breast tumors, leading to an augmentation of the antitumor efficacy when used in combination with ANA.

Materials and methods

Reagents

Tegafur, gimeracil, oteracil, uracil, and ANA were synthesized in our laboratory. S-1 was prepared by mixing tegafur, gimeracil, and oteracil at a molar ratio of 1:0.4:1 in 0.5% hydroxypropyl methylcellulose (HPMC). UFT was prepared by mixing tegafur and uracil at a molar ratio of 1:4 in 0.5% HPMC. 5-Fluorouracil (5-FU) and TXL were purchased from Wako Pure Chemicals Co., Ltd. Testosterone and 17 β -estradiol (E₂) were purchased from Tokyo Chemical Ind., Co., Ltd. and Sigma Chemical Co., respectively. Doxorubicin hydrochloride injection (ADM) and estradiol propionate injection were purchased from Kyowa Hakkō Kirin Co., Ltd. and ASKA Pharmaceutical Co., Ltd., respectively.

Fetal calf serum (FCS) and dextran-coated charcoal-stripped (DCC)-FCS was purchased from JRH Bioscience and Tissue-Culture Bioscience, respectively. Tween[®] 80 and Cremophor[®] were purchased from NACALAI Tesque, Inc. The High-Capacity cDNA Archive Kit, TaqMan gene expression assay primer probe set for ER- α , and glyceraldehyde-3-phosphate dehydrogenase (GAPDH) were purchased from Applied Biosystems Inc. The QuantiTect Probe PCR Kit was purchased from Qiagen.

Anti human ER- α rabbit polyclonal antibody was purchased from Santa Cruz Biotechnology, Inc. All other reagents were commercially available products of the highest grade.

Cell line and transfection

A typical ER- α positive breast cancer cell line, MCF-7, was purchased from the American Type Culture Collection. Full-length cDNA of human aromatase (cytochrome P-19, entry number NM-000103) was purchased from GenBank. The cDNA was ligated into the mammalian expression vector pCI-neo vector (Promega K. K), and the expression vector was then transfected into MCF-7 using FuGENE 6, according to the method described by Yuytersprot et al. [22]. The enzyme activity of aromatase was determined using [³H]-androst-4-ene-3, 17-dione [¹ β -³H (N)], the radioactivity of which was 24 kCi/mmol as a substrate according to the method described by Silva et al. [23].

Cell growth assay in vitro

To reduce endogenous estrogen-like activity, the cells were pre-cultured with phenol-red, which exerts a weak estrogenic activity, free RPM-1640 supplemented with 2.5% DCC-FCS at 37°C under 5% CO₂ and 100% humidity in vitro. The cells were seeded into a 96-multiwell plate on day 0 in the presence or absence of various concentrations of testosterone or E₂ (6 wells/plate, with the reproducibility clarified using five plates). The hormone-dependent cell growth was evaluated according to the reported crystal violet-staining method [24] on day 10 (MCF-7/Arom 14) or day 8 (MCF-7) according to the following formula: Cell growth (% of hormone-free well) = (OD₅₄₀ of hormone-treated well)/(OD₅₄₀ of hormone-free well) \times 100 (%).

To determine the growth inhibitory activities of 5-FU or ANA, various concentrations of 5-FU and ANA were added to the medium in the presence of 3 nM testosterone on the day after cell seeding, and cell growth was evaluated on day 10 according to the following formula: Cell growth (% of control) = (OD₅₄₀ of treated well)/(OD₅₄₀ of control) \times 100 (%).

The combinatory effect of 5-FU and ANA against MCF-7/Arom 14 was evaluated based on the combination index (CI), as described by Chou [25]. MCF-7/Arom 14 was seeded into 96-multi well plates on day 0, ANA and 5-FU were applied in a fixed molar ratio of 1:100 on day 1, and cell growth was evaluated on day 10. The value of CI was calculated based on the growth inhibition ratio using CalcuSyn.

Antitumor activity in vivo

All animal studies were carried out according to the guidelines and with the approval of the institutional animal care and use committee of Taiho Pharmaceutical Co., Ltd. Five-week-old female BALB/c *nu/nu* mice were purchased from CLEA Japan Inc. Mice were housed under specific pathogen-free conditions, and food and water were given ad libitum. After the mice had been in quarantine for 1 week, they were implanted subcutaneously (s.c.) with a 8-mm³ fragment of MCF-7/Arom 14 solid tumor, and estradiol propionate (0.25 mg/body) was administered on the day after tumor implantation. To evaluate the antitumor activity, the mice were divided into seven groups according to the tumor volume once the mean tumor volume reached about 150–200 mm³ (day 0). Each group consisted of 10 mice. Testosterone was mixed with cholesterol and used to prepare the Tes-P so that each pellet contained 2 mg of testosterone according to a previously reported method [26]. The Tes-P was then implanted s.c. at a site contralateral to the tumor on day 0 (s.c.). S-1 (10 mg/kg, p.o.), UFT (20 mg/kg, p.o.), and ANA (3 mg/kg, s.c.) dissolved in saline containing 1% Tween[®] 80 were administered

once daily from days 1 to 21. The maximal tumor diameters were measured twice a week, and the tumor volume was estimated as $0.5 \times \text{Length} \times \text{Width}^2$. The relative tumor volume (RTV) was calculated using the following formula: $\text{RTV} = \text{tumor volume on measured day}/\text{tumor volume on day 0}$. On day 22, the tumor growth inhibition ratio (TGI) was calculated using the following formula: $\text{TGI} = (1 - (\text{mean tumor volume of treated group}/(\text{mean tumor volume of control group})) \times 100 (\%)$. Tumor size was plotted, and the period required for the RTV to reach 3 was estimated using linear regression. The growth delay period (GDP) was calculated using the following formula: $\text{GDP (days)} = (\text{Estimated period required for the mean RTV of the treated group to reach 3}) - (\text{Estimated period for the mean RTV of the control group to reach 3})$, according to the method described by Luo et al. [27].

Immunohistochemical staining for ER- α in tumor tissue

MCF-7/Arom 14-bearing mice were prepared as mentioned above and were divided into five groups once the tumor diameter reached about 1 cm (day 0). Each group consisted of five mice. S-1 (10 mg/kg, p.o.) and ANA (3 mg/kg, s.c.) were administered from days 1 to 7. TXL (15 mg/kg), which was dissolved in saline supplemented with 8.3% Cremophor[®] EL and 8.3% ethanol or ADM (5 mg/kg), was administered intravenously on day 1; this dose has been previously reported to be effective [28, 29]. On day 8, the tumor tissue was collected and divided into two parts to evaluate the protein and mRNA expression levels of ER- α . For the immunohistochemical analysis, partial specimens were fixed in 10% formalin, and paraffin-embedded tissue sections were prepared. Heat-induced antigen retrieval was applied using a pressure cooker at 120°C for 30 s, followed by heating at 90°C for 10 s in pH 6.0. Endogenous peroxidase was inactivated by the application of 0.03% hydrogen peroxide in methanol for 10 min at room temperature. ER- α was stained using anti-human ER- α (1:100 dilution) and HRP-conjugated goat anti-rabbit antibody, with 3,3'-diaminobenzidine tetrahydrochloride solution containing 0.003% hydrogen peroxide used as the substrate. Negative control studies were performed without applying the primary antibodies. All procedures were done using Dako Autostainer University Staining. One slide was prepared for every tumor, and all the samples were analyzed in tetraplicate fields at random without using an unblinded methodology; each group consisted of five slides. Approximately 500–700 cells/field were counted at a magnification of 400 \times except in the necrotic area of the central tumor and the connective tissues or blood vessels of the mice. Sections immunostained for ER- α were classified into three groups according to the staining intensity: (++) highly stained, (+) stained, and (–) not stained.

Real-time reverse transcription (RT)-polymerase chain reaction (PCR) for ER- α in tumor tissue

Total RNA was isolated from the residual part of the tumor tissue, and first-strand cDNA was synthesized from 500 ng of total RNA using the High-Capacity cDNA Archive Kit, as described by the manufacturer, using i-cycler. Real-time RT-PCR was performed using the QuantiTect Probe PCR Kit and ABI PRISM 7900HT Sequence Detection System, according to the manufacturer's instructions. Briefly, 2 ng of cDNA was added to a reaction mixture containing 12.5 μl of 2 \times QuantiTect Probe PCR Master Mix and 1.25 μl of 20 \times TaqMan gene expression assays mix in a final volume of 25 μl . The conditions for real-time RT-PCR were 1 cycle of 50°C for 2 min, 95°C for 15 min; and 40 cycles of 94°C for 15 s and 60°C for 1 min. Gene expression profiling was achieved using the comparative cycle threshold method of relative quantification (the calibrator samples were untreated cells, with GAPDH used as the endogenous control). The Gene Assay IDs of the TaqMan gene expression assay were Hs00174860_m1 for ER- α (ESR1) and Hs99999905_m1 for GAPDH. The relative gene expression levels of ER- α were calculated using the Δ threshold cycle (Ct) method according to the formula shown below. The expression levels of ER- α were expressed as $2^{-\Delta\text{Ct}} \times 100$ for the ease of calculation, where $\Delta\text{Ct} = (\text{Ct of ER-}\alpha) - (\text{Ct of GAPDH})$.

Statistical analysis

The significance of the differences in the mean RTV between the treated and control groups on day 22 was analyzed using the Aspin–Welch two-tailed *t* test. The significances of the differences in mRNA expression and the ratio of highly stained ER- α protein relative to the control were analyzed using \log_2 (ER- α /GAPDH) and a two-tailed Welch *t* test. The combinational effect of ANA and S-1 on the antitumor activity was analyzed using a closed testing procedure and the Aspin–Welch two-tailed *t* test, based on the intersection union-test [30] using EXSAS ver. 7.11 (Arm Systex Co., Ltd., Osaka, Japan).

Results

Aromatase enzyme activity and hormone-dependent growth of aromatase-transfected MCF-7/Arom 14 cells

An aromatase-transfected subline, MCF-7/Arom 14, was established from parental ER-positive MCF-7 cells, which had a less than detectable level of aromatase (2 fmol/mg protein/h). The aromatase activities of MCF-7/Arom 14 in culture and in solid tumor isolated from nude

mice were 453.7 fmol/mg protein/h ($n = 1$) and 111.6 ± 69.6 fmol/mg protein/h ($n = 7$), respectively. In contrast to the parental MCF-7, MCF-7/Arom 14 grew in response to 0.1–10 nM of testosterone. Note that the growth of MCF-7/Arom 14 and the parental cells was stimulated by 0.01–1 nM of E_2 . These data showed that MCF-7/Arom 14 exhibits a level of aromatase activity capable of providing a sufficient amount of E_2 from testosterone to induce cell growth.

Growth inhibitory effect of 5-FU and ANA in vitro

ANA at concentrations of 0.05–10 μ M inhibited the testosterone-induced growth of MCF-7/Arom 14 cells (Figs. 1, 2a). Especially at concentrations of 2–10 μ M, cell growth was equivalent to the hormone-free condition; thus, ANA seemed to cancel the hormone-induced cell growth. 5-FU at concentrations ranging from 0.2 to 10 μ M dose dependently inhibited the growth of MCF-7/Arom 14 cells, and 50 μ M 5-FU completely inhibited cell growth (Fig. 2a). The growth inhibitory effect of ANA in combination with 5-FU was further analyzed using the combination index method. The CI values were approximately 1.0 at various concentration ranges, indicating that the combination of ANA and 5-FU had an additive inhibitory

effect on the testosterone-stimulated growth of MCF-7/Arom 14 cells (Fig. 2b).

Antitumor activity of ANA in combination with oral fluoropyrimidines in vivo

MCF-7/Arom 14 cells administered s.c. survived in nude mice (100%) but did not exhibit stable growth in the absence of Tes-P. The growth of these cells was stimulated by the subcutaneous implantation of Tes-P for several weeks in vivo. The testosterone-stimulated growth of MCF-7/Arom 14 tumors was significantly inhibited by the 21-day consecutive administration of ANA, UFT, or S-1. Moreover, combined treatment with ANA and UFT or S-1 resulted in a significantly potentiated antitumor activity (Fig. 3; Table 1). The antitumor effects were evaluated based on the period required to inhibit tumor growth. The difference of period between controls required for the RTV to reach 3.0, which was regarded as the growth delay period (GDP), was estimated using linear regression based on the tumor volume changes and differences from the control. Drug administration suppressed tumor growth continuously, and the GDP values were 2.4, 3.0, and 5.5 days for ANA, UFT, and S-1, respectively. Interestingly, the GDP values for combined treatment with ANA

Fig. 1 Proliferation of MCF-7/Arom 14 cells (a) and parental MCF-7 cells (b) in the presence of testosterone or estradiol in vitro. Cells were cultured in hormone-free conditions or with testosterone (closed square) or E_2 (open circle) and cell growth was evaluated. The values indicate the means and SD (% of hormone-free conditions, $n = 5$)

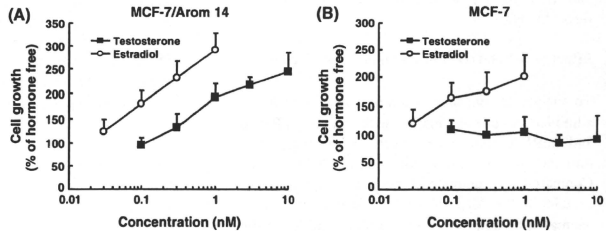
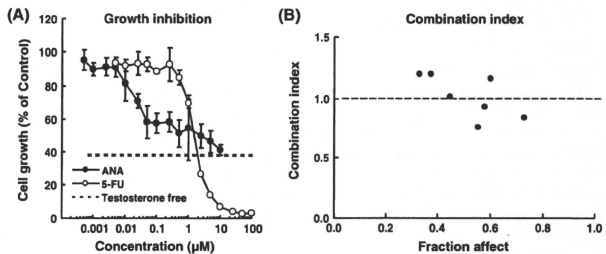


Fig. 2 Growth inhibitory effects of ANA (closed circle) and 5-FU (open circle) in the presence of 3 nM testosterone (control) against MCF-7/Arom 14 cells in vitro. The dotted line indicates cell growth in the absence of testosterone. The values indicate the means and SD of cell growth (% of control, $n = 3$) (a). Combination index (b)



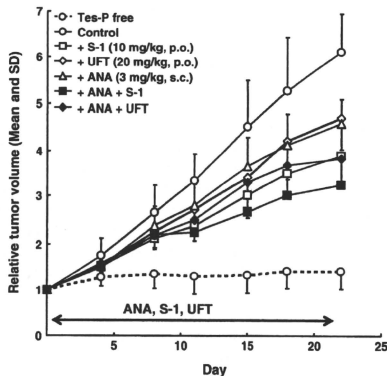


Fig. 3 Tumor volume changes in MCF-7/Arom 14 cells in vivo. Nude mice bearing MCF-7/Arom 14 cells were randomized into seven groups and Tes-P was administered on day 0 (s.c.). ANA (3 mg/kg, s.c.), S-1 (10 mg/kg, p.o.), and UFT (20 mg/kg, p.o.) were administered once daily from days 1 to 21. Tumor volume was measured twice a week until day 22. The values indicate the mean and SD of the RTV ($n = 10$)

and UFT or S-1 were enhanced to 4.3 and 9.5 days, respectively.

Effect of S-1 and other drugs on the expression of ER- α

To analyze the enhanced antitumor activity of ANA when administered in combination with S-1, the ER- α protein and mRNA expression levels were evaluated using immunohistochemical staining and RT-PCR, respectively. Compared with untreated tumors, the expression of ER- α protein in the MCF-7/Arom 14 tumors was apparently decreased by treatment with S-1 alone and in combination with ANA, but not by treatment with ADM or TXL (Fig. 4a, b). We divided ER- α expression in the tumor tissues into three categories: high (++), low (+), and none (-). The proportion of highly ER-stained cells was significantly ($P < 0.05$) lower after treatment with S-1 or S-1 + ANA. In contrast, the treatment of tumors with ANA alone showed a slight increase in the proportion of highly stained cells.

We next measured the expression of ER- α mRNA in MCF-7/Arom 14 tumor tissue treated with S-1 and found that its expression was significantly ($P < 0.05$) lower than that in the control. The changes in the mRNA expression level coincided with the changes in the protein level mentioned above. ER- α mRNA expression increased after treatment with ANA alone or ANA + S-1, but no

significant change was observed when compared with the control. ADM and TXL failed to alter either the protein or mRNA expression levels of ER- α (Fig. 5).

Discussions

Aromatase is known to be present in several human tissues including stroma, adipose, and tumor tissue. Both the systemic aromatase expression and adrenal androgen supply in mice are known to differ from that in humans, and established human cancer cell lines have lower aromatase activities than breast cancer tissues. Therefore, to evaluate the antitumor activity of ANA, we established the MCF-7/Arom 14 cell line, which stably expresses human aromatase in the MCF-7 cell line originating from luminal A breast cancer. The growth of MCF-7/Arom 14 cells was stimulated by both E_2 and testosterone in vitro. In contrast, the growth of MCF-7 cells was stimulated by E_2 , but not by testosterone. As the concentrations of testosterone and E_2 required for proliferative MCF-7/Arom 14 cell growth differed, the added testosterone seemed to be not entirely converted to E_2 ; however, as testosterone-induced growth was confirmed, the MCF-7/Arom 14 cells were thought to be appropriate for evaluating the effects of ANA. Indeed, in vitro, the growth induced by testosterone was completely canceled by an ANA concentration of around 0.1 μ M, which is equivalent to the steady state plasma concentration of ANA in postmenopausal women [31]. The combination of ANA and 75-FU in the presence of 3 nM of testosterone, which is approximately the same as the serum level in postmenopausal women [32], showed an additive effect.

The growth of the MCF-7/Arom 14 cells was highly dependent on testosterone, and these cells could not grow without testosterone, in vivo. In subsequent in vivo experiments, the dose of ANA was fixed at 3 mg/kg, which was shown to yield a maximal antitumor activity (data not shown). Although the dosage of ANA in the present study (3 mg/kg/day) was much higher than that of the clinical dose (1 mg/body/day), the antitumor activity of ANA in the present study was relatively lower. This discrepancy might be due to the difference in aromatase activity in the MCF-7/Arom 14 tumor cells and human breast tumor tissues. Aromatase activity in human breast cancer tissue was reported to range from 2 to 80 fmol/mg protein/h [19], which is lower than that in MCF-7/Arom 14 solid tumors (111.6 fmol/mg protein/h). The clearance half-life of ANA in rats is reported to be 2.7 h and is much shorter than that in patients, which is reported to be about 50 h [33]. The clearance half-life of ANA in mice has not been reported; however, based on data from rats, it is speculated to not be longer than that in humans. Therefore, the higher target enzyme activity and the shorter half-life in mice might

Table 1 Antitumor activity of ANA in combination with S-1 and UFT against MCF-7/Arom 14 in vivo

Group	Dose (mg/kg)	Schedule	RTV on day 22 ^a (mean \pm SD)	TGI ^b (%)	GDP ^c (days)
Tes-P free	-	-	1.43 \pm 0.39	-	NE
Control	-	-	6.11 \pm 0.85	-	-
ANA	3	Days 1-21	4.59 \pm 0.49	24.8	2.4
S-1	10	Days 1-21	3.90 \pm 0.62	36.2	5.5
ANA + S-1	3 + 10	Days 1-21	3.24 \pm 0.50 [#]	47.0	9.5
UFT	20	Days 1-21	4.71 \pm 0.67	23.0	3.0
ANA + UFT	3 + 20	Days 1-21	3.83 \pm 0.53 ^{##}	37.4	4.3

NE not evaluated

Tes-P was administered on day 0 (s.c.). S-1 (10 mg/kg, p.o.), UFT (20 mg/kg, p.o.), and ANA (3 mg/kg, s.c.) were administered from days 1 to 21, once daily. Each group consisted of 10 mice

^a Relative tumor volume (RTV) on day 22 was calculated according to the following formula: RTV = (Tumor volume on day 22)/(Tumor volume on day 0)

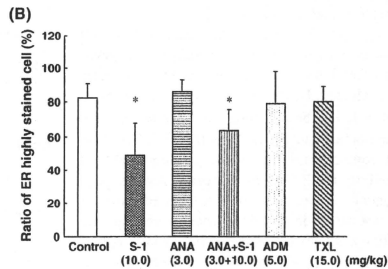
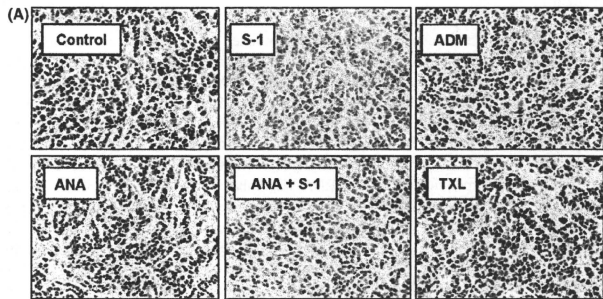
^b Tumor growth inhibition (TGI) was calculated according to the following formula: TGI = [1 - (mean tumor volume of treated group)/(mean tumor volume of control group)] \times 100 (%)

^c Growth delay period (GDP) was calculated according to the following formula: GDP (days) = (Estimated period required for the mean RTV of the treated group to reach 3) - (Estimated period for the mean RTV of the control group to reach 3)

Overall maximal [#] $P < 0.05$ and ^{##} $P < 0.01$ by closed testing procedure using Aspin-Welch t test

Fig. 4 a Immunohistochemical staining for ER- α in MCF-7/Arom 14 solid tumors treated with control, S-1, ADM, ANA, ANA + S-1, and TXL. The original magnification was $\times 400$. **b** Sections immunostained for ER- α were classified into three groups (highly stained, moderately stained, and not stained). The values indicate the mean and SD of the proportions of highly stained cells ($n = 5$).

[#] $P < 0.05$ versus control, Welch t test



limit the antitumor activity of ANA in the present model. Despite this, the antitumor activity of ANA was significantly potentiated by UFT or S-1, suggesting that the

combination of ANA with S-1 or UFT may show promising efficacy for the treatment of postmenopausal patients with breast cancer.

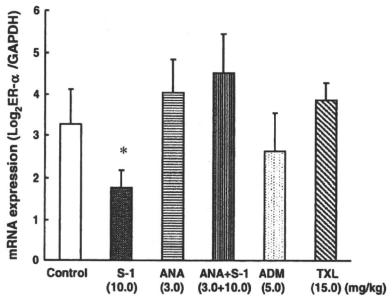


Fig. 5 Change in mRNA levels of ER- α in MCF-7/Arom 14 cells. The mRNA level was detected using real-time reverse transcriptional polymerase chain reaction (RT-PCR) using the TaqMan Real-time RT-PCR system. Values indicate the mean and SD of the relative expression levels of ER- α mRNA normalized by GAPDH ($n = 4$ for ADM, $n = 5$ for controls, S-1, ANA, TXL and ANA + S-1). * $P < 0.05$ versus control, Welch t test

To clarify the mechanism by which S-1 stimulates the antitumor activity of ANA, we took note of the change in the ER- α level, which is the major target of estrogens. As a result, the proportion of cells that stained strongly for ER- α and the mRNA expression levels were significantly ($P < 0.05$) decreased by S-1 and S-1 + ANA, while neither ADM nor TXL decreased the expressions significantly. As the expression of ER- α mRNA was enhanced under estrogen-depressed conditions [34], the response of MCF-7/Arom 14 against ANA for ER- α biosynthesis tended to be appropriate. And a comparison of the ER- α mRNA expression levels with the intensity of immunostaining suggests that ER- α protein expression is not directly dependent on mRNA expression. We attempted to create xenograft models using other ER-positive human breast cancers (T-47D, KPL-1), but unfortunately these cell lines were not tumorigenic *in vivo*. Therefore, ER down-regulation in other luminal A-type human breast cancers could not be evaluated. However, 5-FU, which is an active metabolite of S-1, has been reported to decrease the ER level of human breast cancer cell lines (MCF-7, Br-10) *in vivo* [35, 36]; consequently, ER down-regulation might not be restricted to MCF-7/Arom 14 cells. As the pure estrogen antagonist fulvestrant is used to treat ER-positive metastatic breast cancer in postmenopausal women and its antitumor activity is known to arise mainly from a reduction in ER- α protein [37], ER- α down-regulation is thought to enhance endocrine therapy. A reduction in ER is reportedly correlated with the antitumor activity of fulvestrant *in vivo* [38], and the combination of fulvestrant with ANA is reportedly more active than ANA monotherapy

[39, 40]. Likewise, the reduction of ER- α protein by S-1 might contribute more to the potentiation of the antitumor activity of ANA than the combination with either ADM or TXL, which could not reduce the ER- α protein level. The mechanisms of action responsible for decreasing the ER levels are thought to differ between S-1 and fulvestrant, which accelerates the degradation of ER after binding with estrogen.

The expression of ER- α is reportedly inhibited by estrogen, epidermal growth factor, or insulin-like growth factors [41, 42]; however, it is unlikely that S-1 increases the expression of these factors *in vivo*. While the detailed mechanism of ER- α down-regulation has not yet been clarified, the mechanisms underlying the effects of combination therapy with S-1 and ANA are very important, and we plan to continue studying these mechanisms. In addition to ER down-regulation, the growth inhibitory effects of 5-FU against an ER-positive human breast cancer cell line, KPL-1, were enhanced under E₂-depleted conditions, compared with E₂-supplemented conditions, because of the down-regulation of thymidylate synthase, which is a target enzyme of 5-FU; however, neither the effects of ADM nor TXL were enhanced, as reported by Kurebayashi et al. [43]. As the estrogen-depleted condition mimics the status of postmenopausal patients treated with aromatase inhibitors, the combination of S-1 with ANA, rather than the combination of S-1 with ADM or TXL, might be favorable.

In conclusion, we have shown that S-1 is able to augment the anti-tumor activity of ANA using MCF-7/Arom 14 cells implanted in nude mice and have suggested the possibility that this augmentation is mediated by the down-regulation of ER- α in tumor cells at the transcriptional level. Our present results clinically imply that the combination of oral DIF (S-1 and UFT) and ANA is a promising adjuvant chemoendocrine treatment for postmenopausal patients with luminal A-type breast cancer.

Acknowledgments We thank Prof. J Patrick Barron of the Department of International Medical Communications of Tokyo Medical University for helpful advice and revision of grammatical errors of the manuscript.

References

1. Early Breast Cancer Trialists' Collaborative Group (EBCTCG) (1998) Tamoxifen for early breast cancer: an overview of the randomised trials. *Lancet* 351:1451-1467
2. Early Breast Cancer Trialists' Collaborative Group (EBCTCG) (2005) Effects of chemotherapy and hormonal therapy for early breast cancer on recurrence and 15-year survival: an overview of the randomised trials. *Lancet* 365:1687-1717
3. Albain KS, Barlow WE, Ravdin PM, Farrar WB, Burton GV, Ketchel SJ, Cobau CD, Levine EG, Ingle JN, Pritchard KI, Lichter AS, Schneider DJ, Abeloff MD, Henderson IC, Muss HB, Green SJ, Lew D, Livingston RB, Martino S, Osborne CK, Breast

- Cancer Intergroup of North America (2009) Adjuvant chemotherapy and timing of tamoxifen in postmenopausal patients with endocrine-responsive, node-positive breast cancer: a phase 3, open-label, randomised controlled trial. *Lancet* 374:2055–2063
4. Hayes DF, Thor AD, Dressler LG, Weaver D, Edgerton S, Cowan D, Broadwater G, Goldstein LJ, Martino S, Ingle JN, Henderson IC, Norton L, Winer EP, Hudis CA, Ellis MJ, Berry DA, Cancer and Leukemia Group B (CALGB) Investigators (2007) HER2 and response to paclitaxel in node-positive breast cancer. *N Engl J Med* 357:1496–1506
 5. Spitale A, Mazzola P, Soldini D, Mazzucchelli L, Bordoni A (2009) Breast cancer classification according to immunohistochemical markers: clinicopathologic features and short-term survival analysis in a population-based study from the South of Switzerland. *Ann Oncol* 20:628–635
 6. Goldhirsch A, Ingle JN, Gelber RD, Coates AS, Thürlimann B, Senn HJ (2009) Thresholds for therapies: highlights of the St Gallen International Expert Consensus on the primary therapy of early breast cancer 2009. *Ann Oncol* 20:1319–1329
 7. Noguchi S, Koyama H, Uchino J, Abe R, Miura S, Sugimachi K, Akazawa K, Abe O (2005) Postoperative adjuvant therapy with tamoxifen, tegafur plus uracil, or both in women with node-negative breast cancer: a pooled analysis of six randomized controlled trials. *J Clin Oncol* 23:2172–2184
 8. Park Y, Okamura K, Mitsuyama S, Saito T, Koh J, Kyono S, Higaki K, Ogita M, Asaga T, Inaji H, Komichi H, Kohno N, Yamazaki K, Tanaka F, Ito T, Nishikawa H, Osaki A, Koyama H, Suzuki T (2009) Uracil-tegafur and tamoxifen vs cyclophosphamide, methotrexate, fluorouracil, and tamoxifen in post-operative adjuvant therapy for stage I, II, or IIIA lymph node-positive breast cancer: a comparative study. *Br J Cancer* 101:598–604
 9. Ohashi Y, Watanabe T, Sano M, Koyama H, Inaji H, Suzuki T (2010) Efficacy of oral tegafur-uracil (UFT) as adjuvant therapy as compared with classical cyclophosphamide, methotrexate, and 5-fluorouracil (CMF) in early breast cancer: a pooled analysis of two randomized controlled trials (N-SAS-BC 01 trial and CUBC trial). *Breast Cancer Res Treat* 119:633–641
 10. Toi M, Ikeda T, Akiyama F, Kurosumi M, Tsuda H, Sakamoto G, Abe O (2007) Predictive implications of nucleoside metabolizing enzymes in premenopausal women with node-positive primary breast cancer who were randomly assigned to receive tamoxifen alone or tamoxifen plus tegafur-uracil as adjuvant therapy. *Int J Oncol* 31:899–906
 11. The ATAC (Arimidex Tamoxifen Alone or in Combination) Trialists' Group (2002) Anastrozole alone or in combination with tamoxifen versus tamoxifen alone for adjuvant treatment of postmenopausal women with early breast cancer: first results of the ATAC randomised trial. *Lancet* 359:2131–2139
 12. Kaufmann M, Jonat W, Hilfrich J, Eidmann H, Gademann G, Zuna I, von Minckwitz G (2007) Improved overall survival in postmenopausal women with early breast cancer after anastrozole initiated after treatment with tamoxifen compared with continued tamoxifen: the ARNO 95 Study. *J Clin Oncol* 25:2664–2670
 13. Jonat W, Gnani M, Boccardo F, Kaufmann M, Rubagotti A, Zuna I, Greenwood M, Jakesz R (2006) Effectiveness of switching from adjuvant tamoxifen to anastrozole in postmenopausal women with hormone-sensitive early-stage breast cancer: a meta-analysis. *Lancet Oncol* 7:991–996
 14. Fukushima M, Satake H, Uchida J, Shimamoto Y, Kato T, Takechi T, Okabe H, Fujioka A, Nakano K, Ohshimo H, Takeda S, Shirasaka T (1998) Preclinical antitumor efficacy of S-1: a new oral formulation of 5-fluorouracil on human tumor xenografts. *Int J Oncol* 13:693–698
 15. Sakata Y, Ohtsu A, Horikoshi N, Sugimachi K, Mitachi Y, Taguchi T (1998) Late phase II study of novel oral fluoropyrimidine anticancer drug S-1 (1 M tegafur–0.4 M gimestat–1 M otastat potassium) in advanced gastric cancer patients. *Eur J Cancer* 34:1715–1720
 16. Ohtsu A, Baba H, Sakata Y, Mitachi Y, Horikoshi N, Sugimachi K, Taguchi T (2000) Phase II study of S-1, a novel oral fluoropyrimidine derivative, in patients with metastatic colorectal carcinoma. *Br J Cancer* 83:141–145
 17. Saeki T, Takashima S, Sano M, Noboru Horikoshi N, Miura S, Shimizu S, Morimoto K, Kimura M, Aoyama H, Ota J, Noguchi S, Taguchi T (2002) A phase II study of S-1 in patients with metastatic breast cancer—a Japanese trial by the S-1 Cooperative Study Group, Breast Cancer Working Group. *Breast Cancer* 11:194–202
 18. Miki Y, Suzuki T, Tazawa C, Yamaguchi Y, Kitada K, Honma S, Moriya T, Hirakawa H, Evans DB, Hayashi S, Ohuchi N, Sasano H (2007) Aromatase localization in human breast cancer tissues: possible interactions between intratumoral stromal and parenchymal cells. *Cancer Res* 6:3945–3954
 19. Salhab M, Reed MJ, Al Sarakbi W, Jiang WG, Mokbel K (2006) The role of aromatase and 17- β -hydroxysteroid dehydrogenase type 1 mRNA expression in predicting the clinical outcome of human breast cancer. *Breast Cancer Res Treat* 99:155–162
 20. Sun XZ, Zhou D, Chen S (1997) Autocrine and paracrine actions of breast tumor aromatase. A three-dimensional cell culture study involving aromatase transfected MCF-7 and T-47D cells. *J Steroid Biochem Mol Biol* 63:29–36
 21. Rebar RW, Morandini IC, Erickson GF, Petze JE (1981) The hormonal basis of reproductive defects in athymic mice: diminished gonadotropin concentrations in prepubertal females. *Endocrinology* 108:120–126
 22. Uyttersprot N, Costagliola S, Miot F (1998) A new tool for efficient transfection of dog and human thymocytes in primary culture. *Mol Cell Endocrinol* 142:35–39
 23. Silva MC, Rowlands MG, Dowsett M, Gusterson B, McKinna JA, Fryatt I, Coombes RC (1989) Intratumoral aromatase as a prognostic factor in human breast carcinoma. *Cancer Res* 49:2588–2591
 24. Saotome K, Morita H, Umeda M (1989) Toxicology in Vitro. Cytotoxicity test with simplified crystal violet staining method using microtitre plates and its application to injection drugs. *Toxicol In Vitro* 3:317–321
 25. Chou TC, Talalay P (1977) A simple generalized equation for the analysis of multiple inhibitions of Michaelis-Menten kinetic systems. *J Biol Chem* 252:6438–6442
 26. Wieder R, Shimkin MB (1964) An improved method of producing hormone-cholesterol pellets. *J Natl Cancer Inst* 32:957–958
 27. Luo FR, Yang Z, Dong H, Camuso A, McGlinchey K, Fager K, Fiefeh C, Kan D, Inigo I, Castaneda S, Rose WC, Kramer RA, Wild R, Lee FY (2005) Correlation of pharmacokinetics with the antitumor activity of Cetuximab in nude mice bearing the GEO human colon carcinoma xenograft. *Cancer Chemother Pharmacol* 56:455–464
 28. Newman SP, Foster PA, Stengel C, Day JM, Ho YT, Judde JG, Lassalle M, Prevost G, Leese MP, Potter BV, Reed MJ, Purohit A (2008) STX140 is efficacious in vitro and in vivo in taxane-resistant breast carcinoma cells. *Clin Cancer Res* 14:597–606
 29. Hardman WE, Moyer MP, Cameron IL (1999) Efficacy of treatment of colon, lung and breast human carcinoma xenografts with: doxorubicin, cisplatin, irinotecan or topotecan. *Anticancer Res* 19:2269–2274
 30. Bauer P, Röhmel J, Maurer W, Hothorn L (1998) Testing strategies in multi-dose experiments including active control. *Stat Med* 17:2133–2146
 31. Yates RA, Dowsett M, Fisher GV, Selen A, Wyld PJ (1996) Arimidex (ZD1033): a selective, potent inhibitor of aromatase in postmenopausal female volunteers. *Br J Cancer* 73:543–548

32. Berrino F, Pasanisi P, Bellati C, Venturelli E, Krogh V, Mastroianni A, Berselli E, Muti P, Secreto G (2005) Serum testosterone levels and breast cancer recurrence. *Int J Cancer* 113:499–502
33. Dukes M (1997) The relevance of preclinical models to the treatment of postmenopausal breast cancer. *Oncology* 54(Suppl 2):6–10
34. Berthois Y, Dong XF, Roux-Dossetto M, Martin PM (1990) Expression of estrogen receptor and its messenger ribonucleic acid in the MCF-7 cell line: multiparametric analysis of its processing and regulation by estrogen. *Mol Cell Endocrinol* 74:11–20
35. Ogasawara Y, Doihara H, Shiroma K, Kanaya Y, Shimizu N (1999) Effects of experimental chemoendocrine therapy with a combination of a pure antiestrogen and 5-fluorouracil on human breast cancer cells implanted in nude mice. *Surg Today* 29:149–156
36. Koh J, Shiina E, Hosoda Y, Hashimoto M, Yamamoto O, Sakai S, Kubota T, Enomoto K, Abe O (1990) Changes in the hormone receptors of human breast carcinoma xenografts in nude mice by treatment with cytotoxic agents. *Jpn J Surg* 20:89–96
37. Dauvois S, Danielian FS, White R, Parker MG (1992) Antiestrogen ICI 164, 384 reduces cellular estrogen receptor content by increasing its turnover. *Proc Natl Acad Sci USA* 89:4037–4041
38. Yoneya T, Tsunenari T, Taniguchi K, Kanbe Y, Morikawa K, Yamada-Okabe H, Lee YH, Lee MH, Kwon LS (2009) Effects of CH4893237, a new orally active estrogen receptor downregulator, on breast cancer xenograft models with low serum estrogen levels. *Oncol Rep* 21:747–755
39. Jelovac D, Sabnis G, Long BJ, Macedo L, Golubeva OG, Brodie AM (2005) Activation of mitogen-activated protein kinase in xenografts and cells during prolonged treatment with aromatase inhibitor letrozole. *Cancer Res* 65:5380–5389
40. Johnston SR, Martin LA, Head J, Smith I, Dowsett M (2005) Aromatase inhibitors: combinations with fulvestrant or signal transduction inhibitors as a strategy to overcome endocrine resistance. *J Steroid Biochem Mol Biol* 95:173–181
41. Yang Z, Barnes CJ, Kumar R (2004) Human epidermal growth factor receptor 2 status modulates subcellular localization of and interaction with estrogen receptor alpha in breast cancer cells. *Clin Cancer Res* 10:3621–3628
42. Dupont J, Le Roith D (2001) Insulin-like growth factor 1 and oestradiol promote cell proliferation of MCF-7 breast cancer cells: new insights into their synergistic effects. *Mol Pathol* 54:149–154
43. Kurebayashi J, Nukatsuka M, Sonoo H, Uchida J, Kuniwa M (2010) Preclinical rationale for combined use of endocrine therapy and 5-fluorouracil neither doxorubicin nor paclitaxel in the treatment of endocrine-responsive breast cancer. *Cancer Chemother Pharmacol* 65:219–225

Development of 95-gene classifier as a powerful predictor of recurrences in node-negative and ER-positive breast cancer patients

Yasuto Naoi · Kazuki Kishi · Tomonori Tanei · Ryo Tsunashima ·
Naomi Tominaga · Yosuke Baba · Seung Jin Kim · Tetsuya Taguchi ·
Yasuhiro Tamaki · Shinzaburo Noguchi

Received: 6 May 2010 / Accepted: 18 August 2010
© Springer Science+Business Media, LLC. 2010

Abstract Our aim was to develop an accurate diagnostic system using gene expression analysis by means of DNA microarray for prognosis of node-negative and estrogen receptor (ER)-positive breast cancer patients in order to identify a subset of patients who can be safely spared adjuvant chemotherapy. A diagnostic system comprising a 95-gene classifier was developed for predicting the prognosis of node-negative and ER-positive breast cancer patients by using already published DNA microarray (gene expression) data ($n = 549$) as the training set and the DNA microarray data ($n = 105$) obtained at our institute as the validation set. Performance of the 95-gene classifier was compared with that of conventional prognostic factors as well as of the genomic grade index (GGI) based on the expression of 70 genes. With the 95-gene classifier we could classify the 105 patients in the validation set into a high-risk ($n = 44$) and a low-risk ($n = 61$) group with 10-year recurrence-free survival rates of 93 and 53%, respectively ($P = 8.6e-7$). Multivariate analysis demonstrated that the 95-gene classifier was the most important and significant predictor of recurrence ($P = 9.6e-4$) independently of tumor size, histological grade, progesterone receptor, HER2, Ki67, or GGI. The 95-gene classifier developed by us can predict the prognosis of node-negative and ER-positive breast cancer patients with

high accuracy. The 95-gene classifier seems to perform better than the GGI. As many as 58% of the patients classified into the low-risk group with this classifier could be safely spared adjuvant chemotherapy.

Keywords Breast cancer · Prediction of recurrence · DNA microarray · Hormonal therapy

Abbreviations

ER Estrogen receptor
PR Progesterone receptor
HER2 Human epidermal growth factor receptor 2

Introduction

Currently, one of the most important and urgent clinical questions in breast cancer treatment is how we can identify the subset of patients who can be safely spared adjuvant chemotherapy among node-negative and ER-positive breast cancer patients because these patients show a relatively favorable prognosis when treated with adjuvant hormonal therapy alone. However, about 20% of these patients ultimately develop recurrence by 10 years after surgery. In order to reduce the recurrence rate, most of such patients are currently treated with not only adjuvant hormonal therapy but also adjuvant chemotherapy even though adjuvant chemotherapy is considered to be unnecessary for the majority. It can therefore be said to be of vital importance to predict the prognosis of such patients with high accuracy and to administer adjuvant chemotherapy only to those who are at high risk of relapse.

In daily practice, prognosis of node-negative and ER-positive breast cancer patients is estimated by means of

Y. Naoi · T. Tanei · R. Tsunashima · N. Tominaga ·
S. J. Kim · T. Taguchi · Y. Tamaki · S. Noguchi (✉)
Department of Breast and Endocrine Surgery, Osaka
University Graduate School of Medicine, 2-2-E10 Yamadaoka,
Suita-shi, Osaka 565-0871, Japan
e-mail: noguchi@onsurg.med.osaka-u.ac.jp

K. Kishi · Y. Baba
Central Research Laboratories, Sysmex Corporation,
Kobe, Japan

conventional histological examination of tumor size, determination of histological grade, and with biomarkers such as PR and HER2, but prediction of recurrence with these procedures is still inadequate. Moreover, more reliable and accurate predictors need to be developed for implementation of personalized medicine. In the last decade, several efforts have been made to develop molecular based diagnostic systems on basis of analysis of gene expression profiles of breast tumors. These diagnostic systems include MammaPrint™ [1], Oncotype DX™ [2], and genomic grade index (GGI) [3], all of which employ different platforms for the analysis of gene expression. We have also been involved in the development of a molecular based diagnostic system using a DNA microarray (Affymetrix) which can predict the prognosis of node-negative and ER-positive breast cancer patients treated with adjuvant hormonal therapy alone.

In this paper, we report on the diagnostic system using a DNA microarray we have developed for prognosis prediction. Our diagnostic system is unique in that we have attempted to develop a diagnostic system utilizing a large public data base for gene expression profiles ($n = 549$) as a training set and to validate this diagnostic system with an independent set of Japanese breast cancer patients ($n = 105$) treated at our institute. Since Japanese breast cancer patients reportedly show a more favorable prognosis in comparison with Caucasian breast cancer patients, diagnostic system for prognosis prediction needs to be developed in Japanese breast cancer patients.

We also tried to determine whether the "95-gene classifier" diagnostic system developed was effective than the conventional biomarkers such as ER, PR, HER2, and Ki67 for the prediction of patient prognosis, although the previously reported methods, MammaPrint™, Oncotype DX™, and GGI, were not necessarily compared with all these conventional biomarkers. Ideally, our method should also have been compared with MammaPrint™, Oncotype DX™, and GGI, but differences in the platforms for determination of gene expression profiles prevented us from comparing our system with MammaPrint™ and Oncotype DX™ but we could compare our diagnostic system with GGI since the latter can be determined with a DNA microarray (Affymetrix). We were able to show that our "95-gene classifier" diagnostic system is superior not only to the conventional histological prognostic factors ER, PR, HER2 and Ki67, but also to GGI.

Patients and methods

Patients and tumors

From the previously published microarray data base for breast cancer patients (GSE2034, GSE2990, GSE4922,

GSE6532, GSE7390, GSE9195), we selected the 549 ER-positive and node-negative breast cancer patients who had received no adjuvant therapy or hormonal therapy (TAM) alone, 167 of whom developed recurrences. Using the gene expression data of these 549 patients as a training set, we developed a "95-gene classifier" recurrence prediction system, and applied it to an independent validation set of data for 105 Japanese breast cancer patients to verify the validity of this diagnostic system (details of the method for development of this system are described under "95-gene classifier" Statistics). The 105 patients were consecutively recruited from the patients with node-negative and ER-positive invasive breast cancers who underwent breast conserving surgery followed by radiation therapy or mastectomy and consented to tumor sampling for the study and were treated with adjuvant hormonal therapy alone in our hospital during the period from 1996 to 2005. The median follow-up of these patients was 87 months with a range of 3–126 months. Of these 105 patients, 68 were treated postoperatively with tamoxifen (20 mg/day) or toremifene (40 mg/day), 28 with goserelin (3.75 mg/4 weeks) plus tamoxifen (20 mg/day), and 9 were treated with anastrozole (1 mg/day). Tamoxifen, toremifene, and anastrozole were administered for 5 years or until recurrence if it occurred earlier, while goserelin was administered for 2 years. Twenty-four patients developed recurrences. Patient characteristics are shown in Table 1. Tumor tissues obtained at surgery were snap frozen in liquid nitrogen and kept at -80°C until use. Informed consent regarding the study was obtained from each patient before surgery.

RNA extraction and gene expression profiling

RNA was extracted from tumor tissues obtained at surgery with the aid of the Qiagen RNeasy® mini kit (QIAGEN Sciences, Germantown, MD). RNA (1 μg ; RIN value >6) was used for generation of second-strand cDNA, and cRNA was amplified with the Oligo dT primer, then biotinated and fragmented with One-Cycle Target Labeling and control reagents (Affymetrix, Santa Clara, CA), followed by hybridization to UI33 Plus 2.0 array overnight (17 h) according to the manufacturer's protocol. Finally, the hybridized DNA microarray was fluorescence stained with GeneChip® Fluidics Station 450, and scanned with the GeneChip® Scanner 3000 (both from Affymetrix).

Immunohistological examination

ER, PR, and Ki67 expression in tumor tissues was immunohistochemically examined with a previously described method [4]. ER and PR were defined as positive when 10% or more of the tumor cells were positive (ER: Clone 6F11; Ventana Japan K.K., Tokyo, Japan; PR: Clone 16; SRL Inc.,

Table 1 Clinicopathological characteristics of 105 patients in the validation set

	Number of patients	95-Gene classifier		P
		Low-risk	High-risk	
Median age, years (range)	54 (30–83)			
Postmenopausal	56	37	19	0.10
Histological type				
Infiltrating ductal carcinoma	102	59	43	0.76
Infiltrating lobular carcinoma	3	2	1	
T				
T1	58	37	21	0.20
T2	45	23	22	
T3	2	1	1	
T4	0	0	0	
Histological grade				
1	29	22	7	<0.01
2	62	36	26	
3	14	3	11	
ER				
Positive	105	61	44	
Negative	0	0	0	
PR				
Positive	87	52	35	0.45
Negative	18	9	9	
HER2				
Positive	19	8	11	0.12
Negative	86	53	33	
Ki67				
Positive	19	7	12	0.04
Negative	86	54	32	
Subtype (IHC)				
Luminal A	73	45	28	0.27
Luminal B	32	16	16	

ER estrogen receptor, PR progesterone receptor, HER2 human epidermal growth factor receptor 2, IHC immunohistochemistry, Luminal A ER+ and PR+ and HER2-, Luminal B ER+ and PR+/- and HER2+ or ER+ and PR- and HER2-

Tokyo, Japan). Ki67 was defined as positive when 20% or more of tumor cells stained positive. HER-2 was determined immunohistochemically (Anti-human c-erbB-2 polyclonal antibody; Nichirei Biosciences, Tokyo, Japan) or by means of fluorescence in situ hybridization (FISH) using PathVision Her2 DNA Probe kits (SRL Inc.). When a tumor showed +3 immunostaining or contained more than two genes per cell, it was considered HER2 positive, and the histological grade was determined with the Scarff-Bloom-Richardson grading system [5].

Statistics

Relapse-free survival was measured from the date of surgery to the date of recurrence. In the training set, information on the recurrences was obtained from the public data sets (GSE2034, GSE2990, GSE4922, GSE6532, GSE7390, GSE9195) based on the six papers [3, 6–10]. Recurrences were mostly distant metastases but some local recurrences were included. The detailed information on the recurrent sites is unavailable in these data sets or in the original papers. In the validation set, only distant metastases were included in the recurrences.

Robust multiarray average (RMA) normalization [11] was applied to each of the 549 samples in the training set, and mean expression levels of the set were subtracted in each probe set. The effective size of the probe sets, overlapped between U133A and U133 plus 2.0 array, was calculated by using GeneMeta [12] for the sets of training samples. The sequential forward filtering method, progressing from 5 to 300 probe sets ordered by the rank of the absolute value of the effect size (zScore) stepped by increments of 5 sets, was used to optimize the number of probe sets in the classifier based on between-group analysis (BGA), with assessment of the area under the receiver operating characteristic (ROC) curve obtained with the leave-one-out cross-validation (LOOCV) procedure at each step. The classifier model was then constructed by means of BGA with the optimal number of 95 probe sets from the 549 training samples, and applied to the 105-sample validation set. Recurrence-free survival of high and low risk groups of the validation set were assessed with the Kaplan-Meier plot and log-rank test. Univariate and Multivariate Cox Proportional Hazard analyses were performed for the other clinical factors and the GGI was calculated according to the method of Sotiriou [3].

All statistical analyses were two-sided and $P < 0.05$ was judged to be significant. Hierarchical clustering analysis combined with Spearman's rank correlation coefficient and Ward's method was performed for visualization. Statistical software R (<http://www.R-project.org/>) and Bioconductor packages (<http://www.bioconductor.org/>) were used for all but one step, robust multi-array (RMA)-normalization, for which Affymetrix Expression Console software was used.

Results

Prediction of prognosis using the 95-gene classifier

The diagnostic performance of the 95-gene classifier is summarized in Table 2, showing that 237 of the 549 tumors in the training set were high-risk patients and 312 were low-risk patients, and that 107 of the high-risk and 60

Table 2 Diagnostic accuracy of the 95-gene classifier for the training set and the validation set

	Training set		Validation set	
	Low-risk	High-risk	Low-risk	High-risk
Prognosis				
Recurrence	60	107	4	20
Rec. free	252	130	57	24
NPV (%)	80.8		93.4	
PPV (%)	45.1		45.5	
Sensitivity (%)	64.1		83.3	
Specificity (%)	66.0		70.4	

Rec. recurrence, NPV negative predictive value, PPV positive predictive value

of the low-risk patients developed recurrences. The recurrence-free survival curves in Fig. 1a demonstrate that low-risk patients have a significantly ($P = 5.4e-12$) better prognosis than high-risk patients. The positive predictive value (PPV) of this 95-gene classifier was 45.1%, the negative predictive value (NPV) 80.8%, sensitivity 64.1% and specificity 66.0%. The heat map generated by the hierarchical cluster analysis using our classifier is shown in Fig. 2a.

The 95-gene classifier was then applied to the validation set consisting of 105 Japanese breast cancer patients. Forty-four patients were classified as high-risk and 20 of them developed recurrences, while of the 61 patients classified as low-risk, only 4 developed recurrences. PPV, NPV, sensitivity, and specificity of the 95-gene classifier were 45.5, 93.4, 83.3, and 70.4%, respectively. Recurrence-free survival curves shown in Fig. 1b demonstrate that the low-risk patients showed a significantly ($P = 8.6e-7$) better prognosis than high-risk patients. The 10-year recurrence-free survival rates were 93% for the low-risk and 53% for the high-risk patients. The heat map generated by the

hierarchical cluster analysis of the validation set using the 95-gene classifier is shown in Fig. 2b.

Relationships between risk groups identified by the 95-gene classifier and various clinicopathological parameters

The high-risk group identified with the 95-gene classifier was significantly associated with high histological grade ($P < 0.01$) and Ki67 positivity ($P = 0.04$) (Table 1).

Multivariate analysis for comparison of the 95-gene classifier with other parameters

The results of univariate analysis of the various parameters including GGI are shown in Table 3. A significant association with recurrence was detected for large tumor size, high histological grade, HER2 positivity and high GGI. In addition, the 95-gene classifier was found to be significantly ($P = 5.1e-5$) associated with recurrences. In addition, multivariate analysis demonstrated that the 95-gene classifier, not GGI, was the most important and significant predictor of recurrences ($P = 9.6e-4$).

Discussion

In this study, we attempted to develop an accurate diagnostic system for prognosis by means of gene expression profiling with a DNA microarray. We were able to develop a new "95-gene classifier" diagnostic system for ER-positive and node-negative breast cancer patients. This 95-gene classifier was found to have a high negative predictive value (NPV) of 93.4% and classified as many as about 58% of node-negative and ER-positive tumors in the validation set into the low-risk group. This classifier can thus be expected to be clinically useful for the selection of

Fig. 1 Recurrence-free survival curves of breast cancer patients. Recurrence-free survival curves are shown of patients who were classified into high-risk and low-risk groups in the training set ($n = 549$) (a) and in the validation set ($n = 105$) (b)

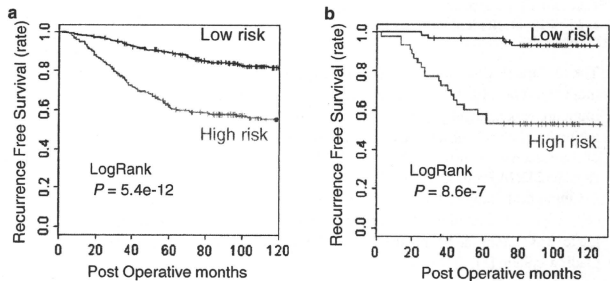
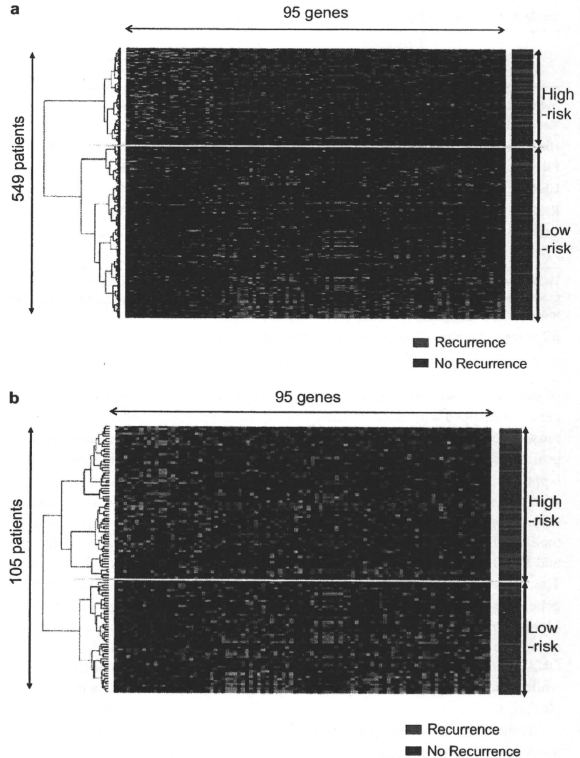


Fig. 2 Hierarchical cluster analysis. Hierarchical cluster analysis was performed for the training set ($n = 549$) (a) and the validation set ($n = 105$) (b), and heat map for each analysis is shown



patients with breast tumors which are very unlikely to recur and can safely be spared adjuvant chemotherapy.

Since prognosis for node-negative and ER-positive breast tumors is usually made on the basis of tumor size, HG, PR, HER2, and, more recently, Ki67, it was deemed important to compare the 95-gene classifier with these conventional prognostic parameters to determine its independent prognostic value. We therefore conducted a multivariate analysis for comparison of the 95-gene classifier with these conventional prognostic factors and were able to demonstrate that the 95-gene classifier is a highly significant prognostic factor independent of the other conventional prognostic factors. In addition, we compared the 95-gene classifier with GGI, which is determined by expression analysis of the 97 genes and which previous

studies have shown to be highly significantly associated with prognosis [3, 13, 14]. In fact, univariate analysis showed that tumors with a high GGI were significantly associated with poor prognosis, but multivariate analysis of various prognostic factors, including both the 95-gene classifier and GGI, made it clear that the former, but not the latter, is an independent prognostic factor. This indicates that the 95-gene classifier is a more reliable predictor of prognosis for node-negative and ER-positive breast cancers.

The 95 genes included in the 95-gene classifier are shown in Table 4. They include the genes related to mitosis and cell cycle proliferation (22), transcription (17), signal transduction (8), apoptosis (8), transport (8), metabolic processes (8), RNA processing and splicing (3), and ATP or GTP (3). Most of these genes (72/95) were up-regulated

Table 3 Univariate and multivariate analysis of various parameters associated with prognosis

	Univariate				Multivariate			
	Hazard ratio	Lower 95	Upper 95	P	Hazard ratio	Lower 95	Upper 95	P
Menopausal status	1.79	0.80	4.04	0.159	1.32	0.55	3.15	0.535
Tumor size	2.49	1.22	5.05	0.012	2.25	1.09	4.64	0.028
Histological grade	2.71	1.08	6.84	0.035	1.24	0.40	3.82	0.705
PR	0.51	0.20	1.30	0.158	0.56	0.20	1.55	0.265
HER2	2.84	1.21	6.65	0.016	2.21	0.88	5.52	0.091
Ki67	1.69	0.67	4.26	0.267	0.65	0.22	1.89	0.429
GGI	2.22	1.45	3.39	2.4E-04	1.08	0.63	1.86	0.780
95-Gene classifier	9.23	3.15	27.07	5.1E-05	7.70	2.29	25.87	9.6E-04

Hazard ratios based on postmenopausal versus premenopausal, large tumor size (>2.0 cm) versus small tumor size, histological grade III versus grade I + II, PR-positive versus PR-negative, HER2-positive versus HER2-negative, Ki67 positive versus Ki67 negative and high GGI versus low GGI

ER estrogen receptor, PR progesterone receptor, HER2 human epidermal growth factor receptor 2

in the patients with recurrence, while 23 genes of the 95 genes overlapped with those included in GGI. Interestingly, most of these genes are implicated in the regulation of cell proliferation. On the other hand, only two genes overlapped with those included in MammaPrintTM and none with those included in Oncotype DXTM. The genes overlapping with those in MammaPrintTM were ECT2 (epithelial cell transforming sequence 2 oncogene, signaling) and PRC1 (protein regulator of cytokinesis 1, cell cycle). The higher percentage of overlapping genes for the 95-gene classifier and GGI than for the 95-gene classifier and MammaPrintTM or Oncotype DXTM is attributable, at least in part, to the fact that the same platform, the Affymetrix DNA microarray, is used for the 95-gene classifier and GGI while MammaPrintTM and Oncotype DXTM use other platforms [15].

MammaPrintTM's high predictive capability for prognosis has been well documented in previous studies of Caucasian breast cancer patients [16]. However, since differences in the biological characteristics of Japanese and Caucasian breast cancers, especially in terms of prognosis, have been reported, MammaPrintTM's predictive capability of prognosis should also be tested for Japanese breast cancer patients. Very recently, MammaPrintTM was actually used for Japanese breast cancer patients with node-negative (ER-positive and ER-negative) tumors. Ishitobi et al. [17] reported that high-risk patients identified by MammaPrintTM showed a worse prognosis than low-risk patients but the difference was not statistically significant. They also report that as many as 80% (82/102) of breast tumors were classified as high-risk, and only 20% (20/102) as low-risk (36.5% of ER-positive patients were classified into the low risk group), meaning that, according to MammaPrintTM, only 20% of the patients could be spared

adjuvant chemotherapy. This in spite of the fact that MammaPrintTM reportedly is capable of classifying as many as about 27–52% of node-negative breast tumors into the low-risk group [16, 18, 19]. Due to the small number of patients analyzed in Ishitobi et al.'s study, it is difficult to draw a conclusion but at least their results seem to indicate the importance of confirming the efficacy for Japanese patients of the performance of a new diagnostic system, which has been developed for Caucasian patients, since Japanese patients are characterized by a relatively better prognosis than Caucasian patients. On the other hand, the 95-gene classifier developed by us seems to be effective regardless race because it was first developed using the data of Caucasian patients and then validated using the data of Japanese patients.

Oncotype DXTM, consisting of a 21-gene expression analysis, is currently commercially available and its use has recently been increasing [2, 20–22]. So far, only two small studies have been reported which tried to validate the performance of Oncotype DXTM for Japanese patients. Both studies seem to suggest that risk prediction with Oncotype DXTM is reproducible in Japanese patients, although it needs to be confirmed by larger future studies. However, an inherent problem of Oncotype DXTM is that it classifies breast tumors into three categories, i.e., high risk, intermediate risk, and low risk, and appropriate adjuvant therapy for intermediate risk patients has yet to be clarified, although a large clinical study, the TAILORx trial, to clarify this issue is now in progress [23, 24].

In conclusion, we were able to develop a 95-gene classifier which can predict the prognosis of node-negative and ER-positive breast cancer patients with a high accuracy of 93.4% NPV and 83.3% sensitivity. The 95-gene classifier seems to perform better than GGI, and it is speculated